Observation of Toroidal Flow Antiparallel to the $\langle E_r \times B_\theta \rangle$ Drift Direction in the Hot Electron Mode Plasmas in the Compact Helical System

K. Ida, T. Minami, Y. Yoshimura, A. Fujisawa, C. Suzuki, S. Okamura, S. Nishimura, M. Isobe, H. Iguchi, K. Itoh, S. Kado, Y. Liang, I. Nomura, M. Osakabe, C. Takahashi, K. Tanaka, and K. Matsuoka

National Institute for Fusion Science, Toki 509-5292, Japan

(Received 7 March 2000)

A toroidal flow antiparallel to the $\langle E_r \times B_\theta \rangle$ drift direction is observed in the hot electron mode plasmas when a large positive electric field and a sharp electron temperature gradient are sustained inside the internal transport barrier in the Compact Helical System. This toroidal flow reaches up to 5×10^4 m/s at the plasma center, and it is large enough to reverse the toroidal flow driven by a tangentially injected neutral beam. These observations clearly show the plasma favors flow in the minimum ∇B direction at the transport barrier.

DOI: 10.1103/PhysRevLett.86.3040 PACS numbers: 52.55.Hc

A spontaneous poloidal flow has been recognized to be important in the confinement of toroidal plasmas, since poloidal flow velocity and radial electric field shear were found to contribute an improvement of plasma confinement in H-mode plasmas [1,2]. The turbulence in the plasma is predicted to be suppressed by a $E \times B$ velocity shear through the mechanism of a nonlinear decorrelation [3,4]. It has been confirmed experimentally that the $\mathbf{E} \times \mathbf{B}$ shearing rate exceeds the growth rate of the turbulence at the transport barrier [5–7]. The toroidal flow has been considered to be determined by the radial transport of momentum driven by neutral beam injection (NBI) with anomalous shear viscosity [8,9]. Although the $\mathbf{E} \times \mathbf{B}$ velocity shear due to the toroidal flow can be important in the plasma core [10], there have been few experiments that demonstrate a spontaneous toroidal flow not driven by NBI in tokamaks [11–14]. It is generally the case in tokamaks that the plasma rotates parallel (antiparallel) to the plasma current for the coinjected (counterinjected) NBI, which corresponds to a positive (negative) radial electric field (E_r) in L-mode plasmas [15]. However, when a negative E_r is produced at the transport barrier, both localized toroidal flow in the counterdirection and localized poloidal flow in the electron diamagnetic direction are observed even for plasmas with coinjected NBI [5,16,17]. These results show the need for detailed measurements of both toroidal and poloidal flow at the transport barrier, where the toroidal flow profile is not determined by the transport of momentum driven by NBI alone. Yet, despite the importance of the coupling between toroidal and poloidal flow, no studies until now have discussed the toroidal flow at the internal transport, where there is a large radial electric field.

In a Heliotron/Torsatron device, there is no toroidal symmetry, and the minimum ∇B trace has a helical structure and helical flow along the minimum ∇B can be expected. The significant difference between tokamaks and Heliotron devices is the relationship between the poloidal field direction and the direction of dominant symmetry. The pitch angle of dominant symmetry is even larger than that of the averaged poloidal field in a Heliotron device, while it is zero due to the toroidal symmetry in tokamaks. This helical flow should change sign depending on the sign of E_r or on the direction of the magnetic field. However, the toroidal flow observed in the L mode in helical plasmas was always parallel to the NBI direction [18,19]. This is because the toroidal flow associated with the ambipolar radial electric field is small compared with the flow due to NBI in most L-mode discharges. In the hot electron mode where the electron thermal transport barrier is established, a large electric field (>10 kV/m) appears in the plasma core [20–22], then toroidal flow associated with the ambipolar radial electric field may overcome the toroidal flow due to NBI. In this paper, the first observation of toroidal flow antiparallel to the $\langle E_r \times B_\theta \rangle$ drift direction (also antiparallel to the neutral beam injection) near the electron transport barrier in the hot electron mode plasmas is described.

The Compact Helical System (CHS) [23] is a Heliotron/Torsatron device (poloidal period number $L = 2$, and toroidal period number $M = 8$) with a major radius $R_0 = 1$ m, an average minor radius $a = 20$ cm, and a rotational transform $\iota = [\langle RB_\theta / rB_\phi \rangle]$ is 0.3 (center)–1.0 (edge), where R and r are the major and minor radii, B_θ and B_ϕ are the poloidal and toroidal magnetic fields, and $\langle\ \rangle$ denotes a magnetic flux average. The plasma is produced initially by electron cyclotron heating (ECH) (53.2 GHz ECH with short pulse) with hydrogen gas and sustained with a hydrogen neutral beam tangentially injected. The magnetic field strength is 0.88 T and the major radius of the magnetic axis is $R_{ax} = 0.92$ m in this experiment. Radial profiles of ion temperature and both toroidal and poloidal flow velocity are measured with 30 points poloidal and 16 points toroidal charge exchange spectroscopy (CXS) using fully stripped carbon with the time resolutions of 20 ms.

The reversal of toroidal flow is observed when the second ECH pulse ($t = 60$–140 ms, $P_{ECH} = 0.11$ MW)

 0031-9007/01/86(14)/3040(4)$15.00

is applied to the NBI plasma ($t = 40$–200 ms, $E_{\mathrm{NBI}} = 36$ kV, $P_{\mathrm{NBI}} = 0.7$ MW) with low electron density below 0.7×10^{19} m^{-3}, as shown in Fig. 1. Here, ρ is the normalized averaged minor radius ($\rho \approx r/a$). The plasma parameters for the discharges without the second ECH pulse are also plotted as a reference. The electron temperature increases up to 2 keV (hot electron mode), while it is only 0.2 keV when there is no second ECH pulse as seen in Fig. 1(d), which indicates a significant improvement in electron transport. In the hot electron mode plasma, there is no clear evidence of high energy electrons, which should be negligible if any, as seen in the energy spectrum of x-rays measured with a soft x-ray charged coupled device (SX-CCD) camera. The electron temperatures derived from x-ray spectra by assuming Maxwellian distribution in the energy range from 2 to 8 keV are consistent with that measured with 24 points yttrium aluminum garnet (YAG) Thomson scattering. Although the electron temperature dramatically increases at the transition from L mode to hot electron mode, the ion temperature is almost constant [$T_i(0) = 0.27$ keV in the hot electron mode and $T_i(0) = 0.26$ keV in the L mode], which suggests that there is no significant improvement of ion transport in the hot electron mode. The magnitude of the carbon diamagnetic flow is on the order of 1 km/s at $\rho = 0.5$ both for the discharges with and without a second ECH pulse. The electron density measured with YAG Thomson scattering drops to 0.3×10^{19} m^{-3} from 0.5×10^{19} m^{-3} after the second ECH pulse is applied even with constant gas puff, which is due to the effect of pump out by ECH. On the other hand, when there is no second ECH pulse, electron density tends to increase in time even without gas puffing. (Gas puff is turned off at the start of NBI of $t = 40$ ms.) During the second ECH pulse, the electron collisionality is low enough to make the plasma be in the electron root (positive electric field), which is consistent with the neoclassical prediction. The positive radial electric field is mainly contributed by the poloidal flow in the direction parallel to the $\langle E_r \times B_\phi \rangle$ drift. The Lorenz forces due to the toroidal flow and the force due to the ion pressure are negligible in the radial force balance [24]. The Lorenz force due to the poloidal flow is almost balanced with the force due to the radial electric field, and therefore the magnitude of E_r is roughly equal to $v_\theta B_\phi$ in CHS plasmas. The radial electric field derived from plasma

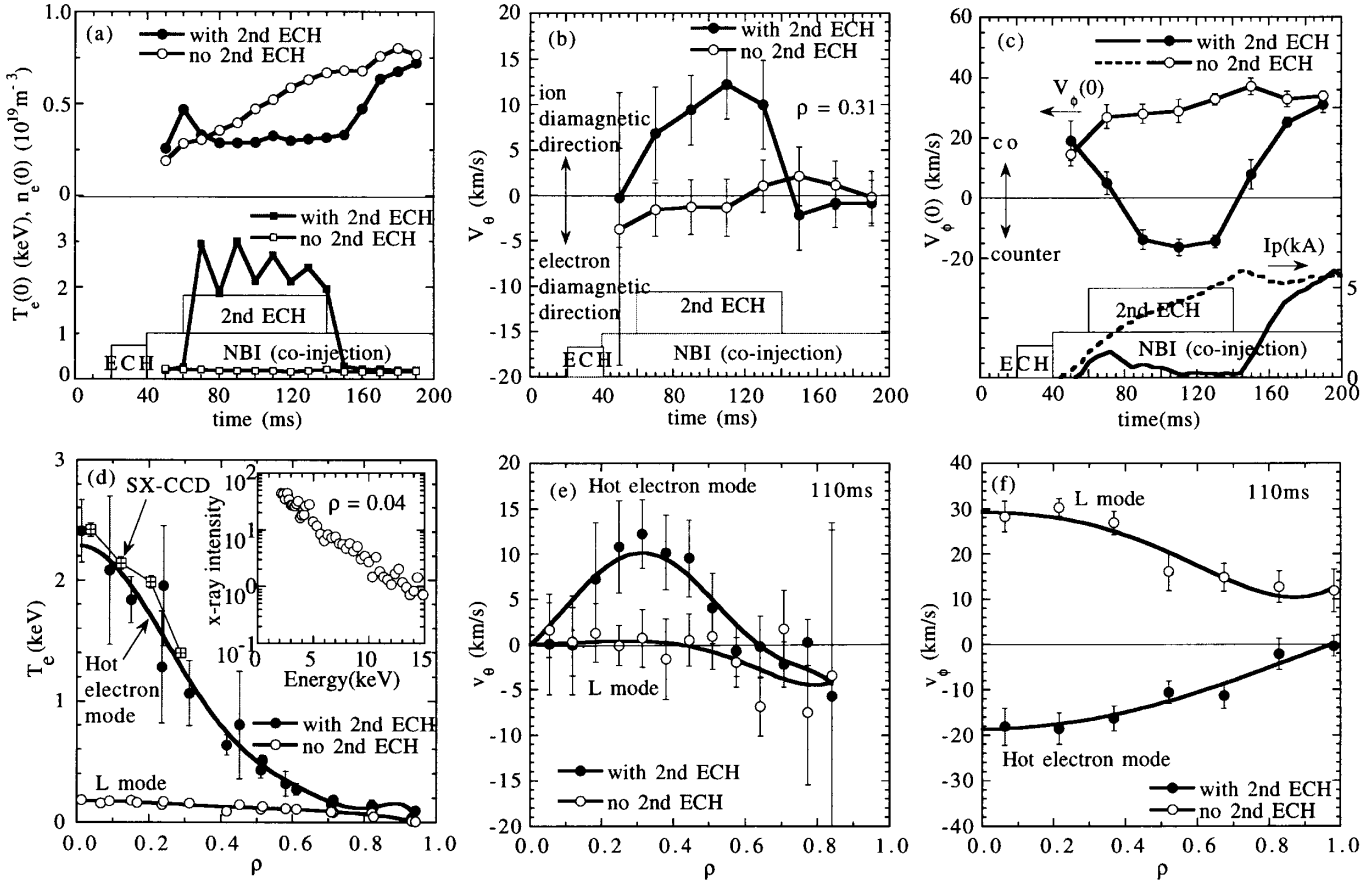

FIG. 1. Time evolution of (a) central electron temperatures and densities, (b) poloidal flow velocity at $\rho = 0.38$, (c) central toroidal flow velocity and toroidal plasma current and radial profiles of (d) electron temperature averaged over 70–140 ms measured with YAG Thomson scattering and a spectrum of x-ray emission at $\rho = 0.04$ and electron temperature measured with a SX-CCD camera, (e) poloidal flow velocity at $t = 110$ ms, and (f) toroidal flow velocity at $t = 110$ ms for the discharges with (solid circles) and without (open circles) second ECH pulse.

flow with the radial force balance agrees well with that measured with a heavy ion beam probe (HIBP) [25]. The large electric field of 10–20 kV/m and the large poloidal flow of 10–20 km/s are produced near the plasma center ($\rho = 0.3$) [Fig. 1(b)], where the sharp temperature gradient is observed [Figs. 1(d) and 1(e)]. According to the HIBP measurements, the radial electric field jumps to positive values within a few microseconds after the onset of the ECH pulse.

The neutral beam is injected to the plasma tangentially in the codirection. Here, the "co" direction (positive flow velocity) is defined as parallel to the equivalent toroidal plasma current, which would produce the average transform actually produced by the external coil current. The "counter" direction (negative flow velocity) is defined as antiparallel to the equivalent toroidal plasma current. As seen in Fig. 1(c), plasma rotates parallel to the NBI when there is no second ECH. This is simply because the toroidal momentum from the NBI causes the plasma toroidal flow. However, when the second ECH is turned on, the toroidal flow velocity decreases and, finally, the plasma rotates antiparallel to the NBI. These measurements clearly show the driven toroidal flow associated with a large poloidal flow (and large positive radial electric field) during the second ECH pulse. The driven toroidal flow reaches 5×10^4 m/s at the plasma center, and it is large enough to overcome the toroidal flow driven by a tangentially injected neutral beam. It should be emphasized that the direction of the toroidal flow is antiparallel to the direction of $\langle E_r \times B_\theta \rangle$ drift. This fact has not been predicted before, because a simple analogy from the experiments in tokamaks implies that the direction of the toroidal flow associated with a large radial electric field is parallel to the direction of $\langle E_r \times B_\theta \rangle$ drift [5,16,17]. This is because the toroidal viscosity is nearly zero due to the toroidal symmetry, and the direction of the toroidal flow is simply determined by the direction of the $\langle E_r \times B_\theta \rangle$ drift in most discharges in tokamaks. It should be noted that the change of toroidal flow shows a relatively long time constant of 20–40 ms, while poloidal flow velocity jumps from ion root to electron root to ion root responding to the second ECH pulse. These differences in the response time scale of the poloidal and toroidal flow are more visible after the second ECH pulse is turned off. The mechanism causing the differences in the response time is unclear. The toroidal plasma current in Fig. 1(c) is net toroidal current including beam driven current (in the codirection) and bootstrap current. When the second ECH is applied, the toroidal plasma is almost zero, while it is 5 kA in the codirection when there is no second ECH. These behaviors of toroidal plasma current suggest that the bootstrap current during the second ECH pulse is in the counterdirection and the magnitude is comparable to that of beam driven current.

The transition from ion root (negative poloidal flow velocity) to electron root (positive poloidal flow velocity) appears at the central electron density of 0.7×10^{19} m^{-3}. As the electron density is decreased, the transition from the L mode to the hot electron mode takes place at the central electron density of 0.5×10^{19} m^{-3}. In the hot electron mode, a large electron temperature gradient up to 60 keV/m is obtained, while it is less than 1 keV/m in the L-mode ion root even with the second ECH pulse, which shows a good correlation to the poloidal flow [Figs. 2(a) and 2(b). Associated with the transition from the L mode to the hot electron mode, the electron energy confinement is improved due to the large E_r shear [26], and the large positive E_r is sustained by the bipolar flux driven by the large electron temperature gradient. The reversal of central toroidal flow is observed clearly when the plasma enters the hot electron mode as shown in Fig. 2(c), because electron temperature gradient and radial electric field become large and the resulting toroidal torque becomes large enough to overcome the torque due to NBI. When there is no second ECH pulse, the poloidal and toroidal flow velocities are almost constant in the wide range of electron density of $0.3–1.5 \times 10^{19}$ m^{-3} [see open circles in Fig. 2(c)].

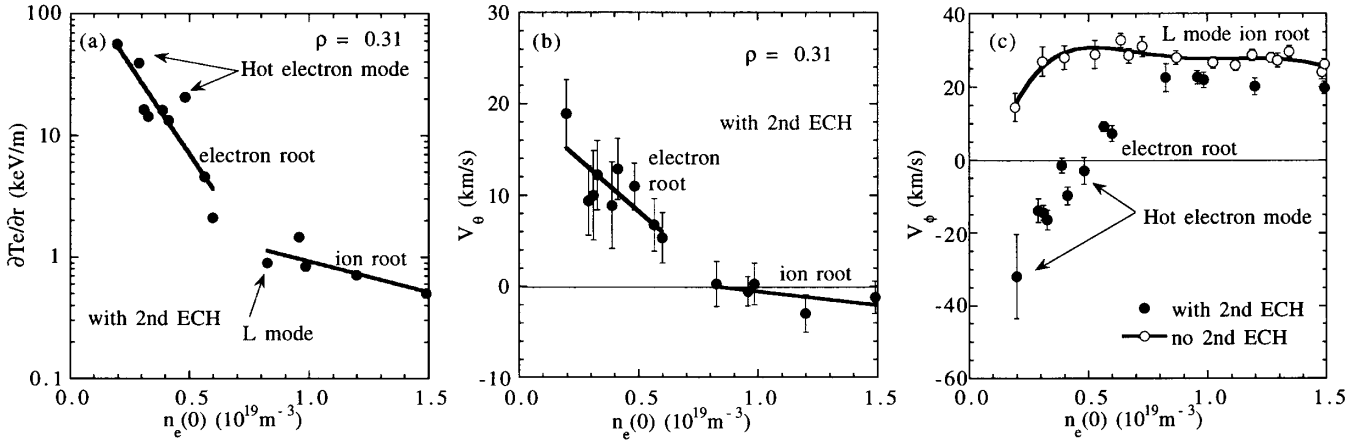

FIG. 2. (a) Gradient of electron temperatures, (b) poloidal flow velocity at $\rho = 0.3$, and (c) central toroidal flow for the discharges with second ECH pulse as a function of central electron density. The central toroidal flow for the discharges without second ECH pulse is also plotted in (c) as a reference.

The plasma flow perpendicular to the magnetic field is strongly coupled with the radial electric field through radial force balance, while the plasma flow parallel to the magnetic field is independent from radial electric field. Since the viscosity favors flow in the minimum grad B direction, flow in other directions will be more strongly damped. Then the toroidal (V_ϕ) and poloidal (V_θ) flow velocities are simply expressed by $V_\theta = E_r \sin\beta/[B\sin(\beta - \alpha)]$ and by $V_\phi = -E_r \cos\beta/B\sin(\beta - \alpha)$, where E_r is the radial electric field, B is the magnetic field, α is the pitch angle of magnetic field B (angle of magnetic field respect to the toroidal direction), and β is the pitch angle of minimum ∇B direction (angle of minimum ∇B direction with respect to the toroidal direction), respectively. As shown in Fig. 3, the β values increase towards the plasma edge and vary along the toroidal direction. The β averaged over the magnetic flux surface, $\langle\beta\rangle$, is approximately $\tan^{-1}[(Mr)/(LR)]$. On the other hand, the pitch angle of the magnetic field, α, changes its sign along the toroidal direction ($\alpha < 0$ at the vertically elongated cross section and $\alpha > 0$ at the horizontally elongated cross section) but smaller than the pitch angle of the minimum ∇B direction, $(\beta - \alpha) > 0$. The plasma flows are measured at the vertical elongated cross section where $\alpha < 0$. The parallel viscosity coefficient in the toroidal direction is on the order of a few tens per millisecond at $\rho = 0.5$. In the hot electron mode plasma, there must be a toroidal stress, perhaps due to the poloidal flow to overcome the force due to the neutral beam injected tangentially. The formula of toroidal flow qualitatively explains the reversal of the sign of V_ϕ between CHS and tokamak plasmas, because $\alpha < \beta$ in Heliotron and $\alpha > \beta = 0$ in tokamak. Then the toroidal velocity is simply proportional to the poloidal velocity ($v_\phi = 16 v_\theta$ at $\rho = 0.3$) if the plasma flows in the direction of $\tan\beta$, in which the parallel viscosity becomes minimum. As seen in Fig. 1(f), the toroidal rotation velocity measured is much smaller than that expected from this relation. This is due to the toroidal force driven by the NBI in the opposite direction and due to the turbulence driven perpendicular viscosity in the diffusion process.

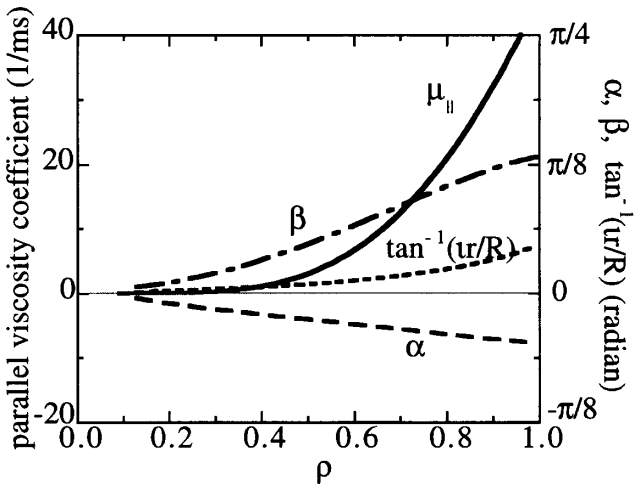

FIG. 3. Radial profiles of parallel viscosity coefficient ($\mu_\parallel$), pitch angle of the minimum ∇B direction (β), and the pitch angle of the magnetic field (α) on the outer side ($R > R_{ax}$) of the midplane in the vertically elongated cross section, calculated with a finite-beta three-dimension equilibrium code VMEC. The profile of $\tan^{-1}(\iota r/R)$ is plotted in (a) as a reference for magnetic flux averaged α.

In conclusion, the toroidal flow antiparallel to the $\langle E_r \times B_\theta\rangle$ drift direction is observed (although the toroidal flow measured is parallel to the direction of the local $E_r \times B_\theta$ drift) in the hot electron mode in CHS. This is in contrast to the spontaneous toroidal flow in the direction parallel to the direction of $\langle E_r \times B_\theta\rangle$ drift in tokamak plasmas [16]. This toroidal flow can be large enough to overcome the toroidal flow driven by a tangentially injected neutral beam at the transport barrier. The reversal of the toroidal flow velocity with the second ECH pulse in the hot electron mode can be explained by the viscous stress, which favors flow in the minimum ∇B direction.

[1] R. J. Groebner, K. H. Burrell, and R. P. Seraydarian, Phys. Rev. Lett. **64**, 3015 (1990).
[2] K. Ida *et al.,* Phys. Rev. Lett. **65**, 1364 (1990).
[3] H. Biglari, P. H. Diamond, and P. W. Terry, Phys. Fluids B **2**, 1 (1990).
[4] K. C. Shaing, E. C. Crume, Jr., and W. A. Houlberg, Phys. Fluids B **2**, 1492 (1990).
[5] K. H. Burrell, Phys. Plasmas **4**, 1499 (1997).
[6] E. J. Synakowski *et al.,* Phys. Rev. Lett. **78**, 2972 (1997).
[7] H. Shirai *et al.,* Nucl. Fusion **39**, 1713 (1999).
[8] S. D. Scott *et al.,* Phys. Rev. Lett. **64**, 531 (1990).
[9] A. Kallenbach *et al.,* Nucl. Fusion **30**, 4645 (1990).
[10] T. H. Osborne *et al.,* Plasma Phys. Controlled Fusion **26**, A237 (1994).
[11] K. Nagashima, Y. Koida, and H. Shirai, Nucl. Fusion **34**, 449 (1994).
[12] K. Ida *et al.,* Phys. Rev. Lett. **74**, 1990 (1995).
[13] K. Ida *et al.,* J. Phys. Soc. Jpn. **67**, 4089 (1998).
[14] J. E. Rice *et al.,* Nucl. Fusion **38**, 75 (1998).
[15] G. A. Hallock *et al.,* Phys. Rev. Lett. **56**, 1248 (1986).
[16] Y. Koide *et al.,* Phys. Plasmas **4**, 1623 (1997).
[17] R. E. Bell *et al.,* Phys. Rev. Lett. **81**, 1429 (1998).
[18] K. Ida, H. Yamada, H. Iguchi, K. Itoh, and CHS Group, Phys. Rev. Lett. **67**, 58 (1991).
[19] J. V. Hofmann *et al.,* in *Proceedings of the 21st European Conference on Controlled Fusion and Plasma Physics, Montpellier, 1994* (IOP, Bristol, 1994), Vol. 18B, Pt. I, p. 392.
[20] A. Fujisawa *et al.,* Phys. Rev. Lett. **82**, 2669 (1999).
[21] J. Baldzuhm *et al.,* Plasma Phys. Controlled Fusion **40**, 967 (1998).
[22] M. Kick *et al.,* Plasma Phys. Controlled Fusion **41**, A549 (1999).
[23] S. Okamura *et al.,* Nucl. Fusion **39**, 1337 (1991).
[24] K. Ida *et al.,* Phys. Fluids B **3**, 515 (1991).
[25] K. Ida *et al.,* Phys. Plasmas **8**, 1 (2001).
[26] T. Minami *et al.,* in *Proceedings of the 26th European Conference on Controlled Fusion and Plasma Physics, Masstricht, 1999* (IOP, Bristol, 1999), Vol. 23J, p. 1357.